REPORT DOCUMENTATION PAGE

Form Approved
OMB No. 0704-0188

1. AGENCY USE ONLY (Leave blank)	2. REPORT DATE	3. REPORT TYPE AND DATES COVERED
	10-19-94	Annual Technical 9/30/93 - 9/29/94

4. TITLE AND SUBTITLE

Compact Free Electron Lasers for Medical Applications

5. FUNDING NUMBERS

N00014-90-J-4130

s400091scu01

6. AUTHOR(S)

Prof. George Bekefi

7. PERFORMING ORGANIZATION NAME(S) AND ADDRESS(ES)

Research Laboratory of Electronics
Massachusetts Institute of Technology
77 Massachusetts Avenue
Cambridge, MA 02139

AD-A285 739

9. SPONSORING/MONITORING AGENCY NAME(S) AND ADDRESS(ES)

Office of Naval Research
800 North Quincy Street
Arlington, VA 22217

408

94-32978

11. SUPPLEMENTARY NOTES

The view, opinions and/or findings contained in this report are those of the author(s) and should not be construed as an official Department of the Army position, policy, or decision, unless so designated by other documentation.

12a. DISTRIBUTION/AVAILABILITY STATEMENT

Approved for public release; distribution unlimited.

12b. DISTRIBUTION CODE

13. ABSTRACT *(Maximum 200 words)*

Work by Prof. Bekefi and his collaborators is summarized here

14. SUBJECT TERMS			15. NUMBER OF PAGES
			16. PRICE CODE
17. SECURITY CLASSIFICATION OF REPORT	18. SECURITY CLASSIFICATION OF THIS PAGE	19. SECURITY CLASSIFICATION OF ABSTRACT	20. LIMITATION OF ABSTRACT
UNCLASSIFIED	UNCLASSIFIED	UNCLASSIFIED	UL

Compact Free Electron Lasers for Medical Applications

Annual Technical Report
Grant No. N00014-90-J-4130
September 30, 1993 - September 29, 1994

R. Stoner, J. Blastos, D. Sisson and G. Bekefi

Submitted October 19, 1994

Short-period (1-10 mm) wigglers for free electron laser (FEL) applications have been a subject of considerable interest. The use of such microwigglers permits higher frequency radiation to be generated with a device which is more compact than one employing wigglers of standard periodicity (typically 3-10 cm). This comes from the fact that the radiation wavelength is proportional to the wiggler period and inversely proportional to the square of the electron beam energy.

The MIT microwiggler program is part of the MIT/ATF collaborative effort to produce a visible and ultraviolet free electron laser. It is a 70-period device consisting of 280 electromagnets wound on ferromagnetic cores. The wiggler [Figure 1] has an 8.8 mm period, 4.2 mm gap, and produces a 0.5 msec long magnetic field pulse of 4 kG and at a repetition rate of 3/4 Hz. There are four electromagnets in each period of the wiggler held in place by a precisely formed aluminum matrix as illustrated in the top photograph of Fig. 1. A WR28 stainless steel waveguide runs through the center of the wiggler and acts as the wiggler bore. The ends of the wiggler field profile have been tapered so as to produce a smooth entry and exit for the electron beam. The entire system is energized by a computer controlled capacitor bank.

Field amplitude tunability, as a means of compensating for random field errors resulting from imperfections in fabrication, becomes increasingly important at short

wavelengths. Field amplitude tunability is also very useful if field tapering is desired; such tapering is known to lead to greatly improved FEL efficiency. In our device, the field of each half-period is independently adjustable via a novel tuning method by which a 0.12% field amplitude uniformity has been achieved. As shown in Fig. 2, the before and after field profiles demonstrate outstanding tunability of this wiggler. Each one of the electromagnets receives current from the bus bar through a resistive wire. By manipulating the length of the wire, we can change the amount of current applied to each magnet and thus tune the wiggler. An axially movable $\dot{B}$ magnetic field probe measures the magnetic field. After the measurements are processed the lengths are adjusted to achieve the desired uniformity. The field uniformity of 0.12% was achieved after only a few iterations of this procedure.

We have installed the wiggler on Beamline #3 at the ATF rf linac. To date, we studied the wiggler's incoherent emission using a 41 MeV beam. The emitted radiation travels from the experimental hall into the FEL room through a series of light-tight fixtures which incorporate a series of mirrors and lenses. The optical transport system is 12 meters in length with no magnification at the output and is optimized for operation for wavelengths of 550 nm. A green HeNe laser is used to align the wiggler center and the light transport optics. Inside the FEL room exists measuring equipment, such as photomultipliers, a spectrometer, and oscilloscopes. All measurements and control operations are conducted inside the FEL room.

The emitted radiation increases with wiggler strength as is illustrated in Fig. 3. The intensity apparently increases linearly with magnetic field rather than as the square of the

field strength as expected. However, this discrepancy may well be due to low signal to noise and electron beam misalignment with the wiggler axis.

The spectrum of the spontaneously emitted light is illustrated in Figure 4. The spectrum has a long shoulder to the red side, which is an indication of the combined effects of beam emittance and the finite solid angle of our light collection optics. After improvements, we expect that such studies of spontaneous emission may well serve as a useful diagnostic of electron beam emittance.

Installation of the optical cavity to achieve lasing will begin shortly. The resonating cavity mirrors for the FEL are on hand. The cavity length will be 3.67m and will be adjustable for tuning purposes. The parabolic cavity mirrors are 5" in diameter. The ATF will produce a hundred 6 psec pulses per macropulse. Outcoupling of the laser light occurs at the upstream side of the wiggler where the light will be redirected to the FEL room via the optical transport system.

Upgrade of the ATF and improved beam characteristics will yield higher brightness and lower emittance leading to a vastly improved spectrum of the spontaneous emission. Concurrent with the ATF modifications, improvements to the wiggler are also underway. These include making an improved capacitor bank, installing mounting tables and resonance cavity mirrors, and optimizing the optical transport systems. We anticipate lasing in the 550 nm range this year.

Detailed description of the completed microwiggler is given in the Appendix.

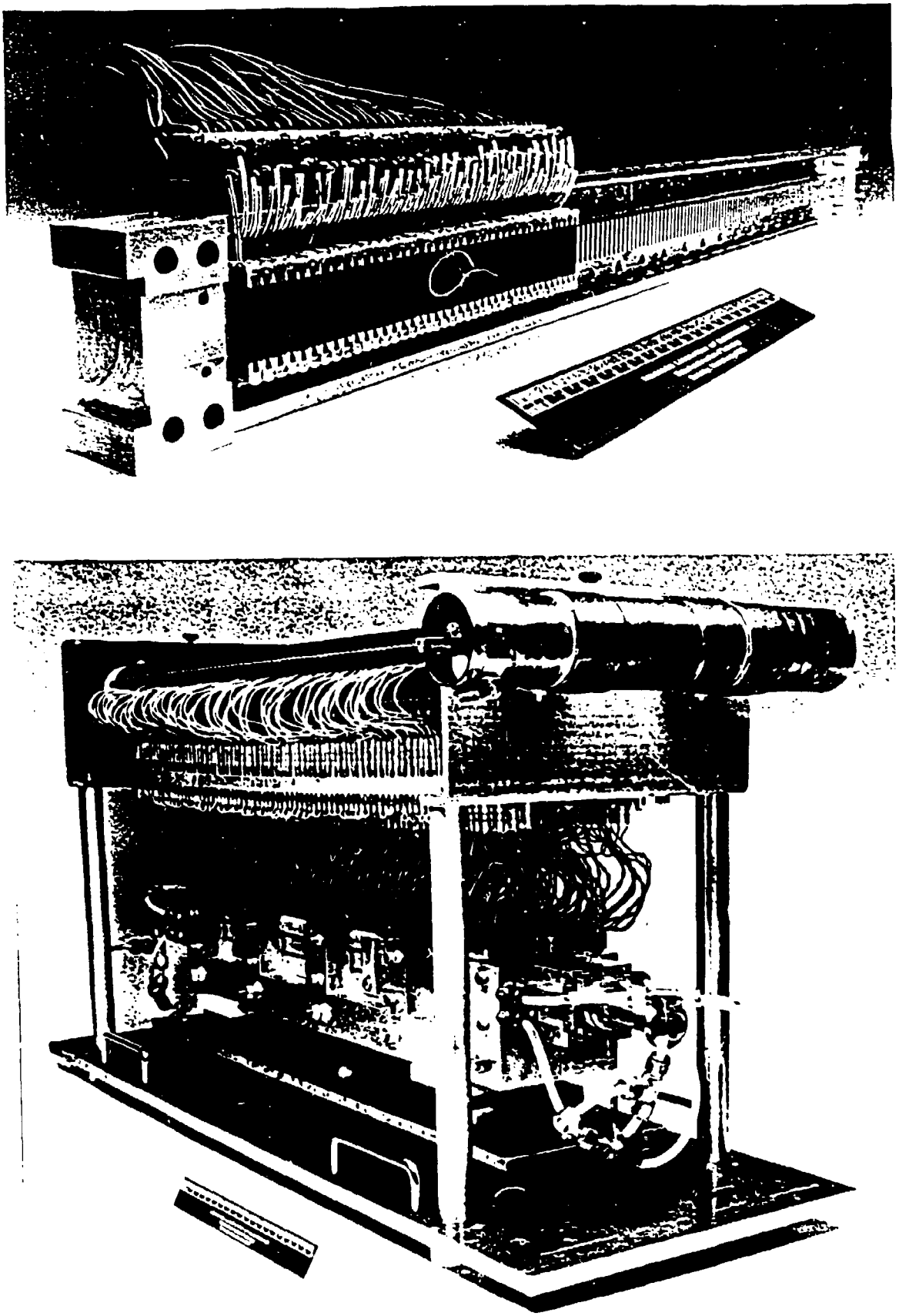

Figure 1 The MIT Microwiggler Cross Section (above); Microwiggler Assembly (below)

Figure 2 Plots showing the magnitude of the peak amplitude of the individual half-periods in the magnet. The top graph is the peak amplitude profile before tuning the magnet. The bottom is the peak amplitude profile after the magnet was tuned.

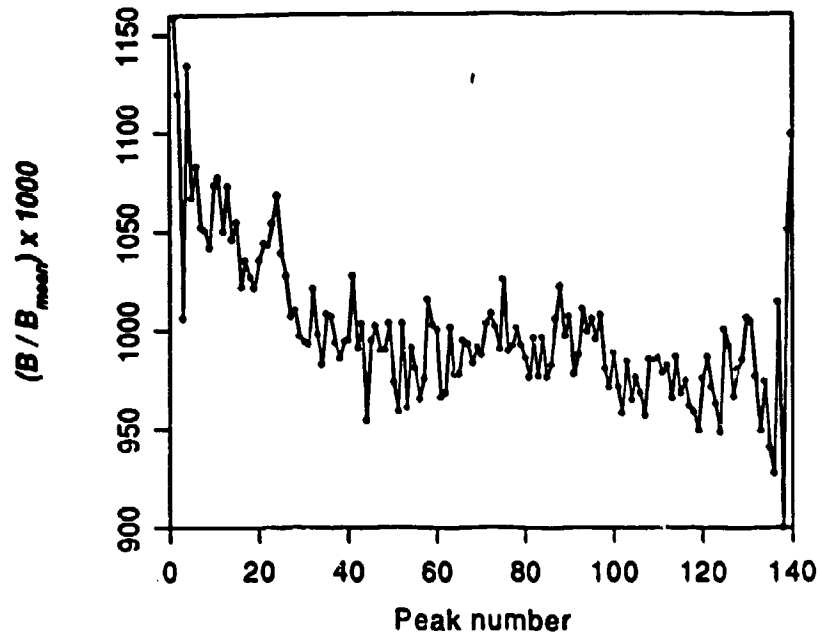

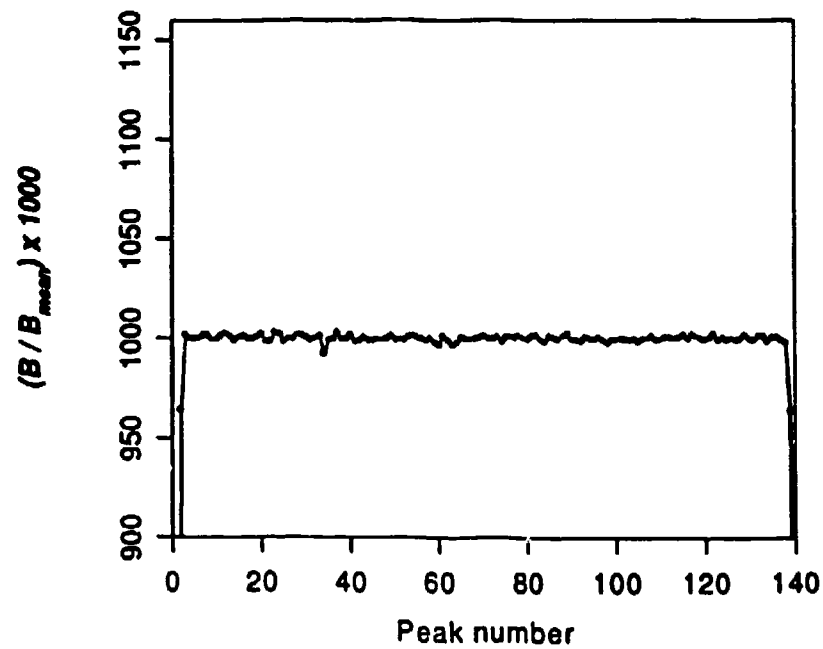

Figure 3 *Plot of the spontaneous emission signal obtained with various values of the wiggler field strength. The open circles correspond to data points taken, the dotted line is a best linear fit to the data.*

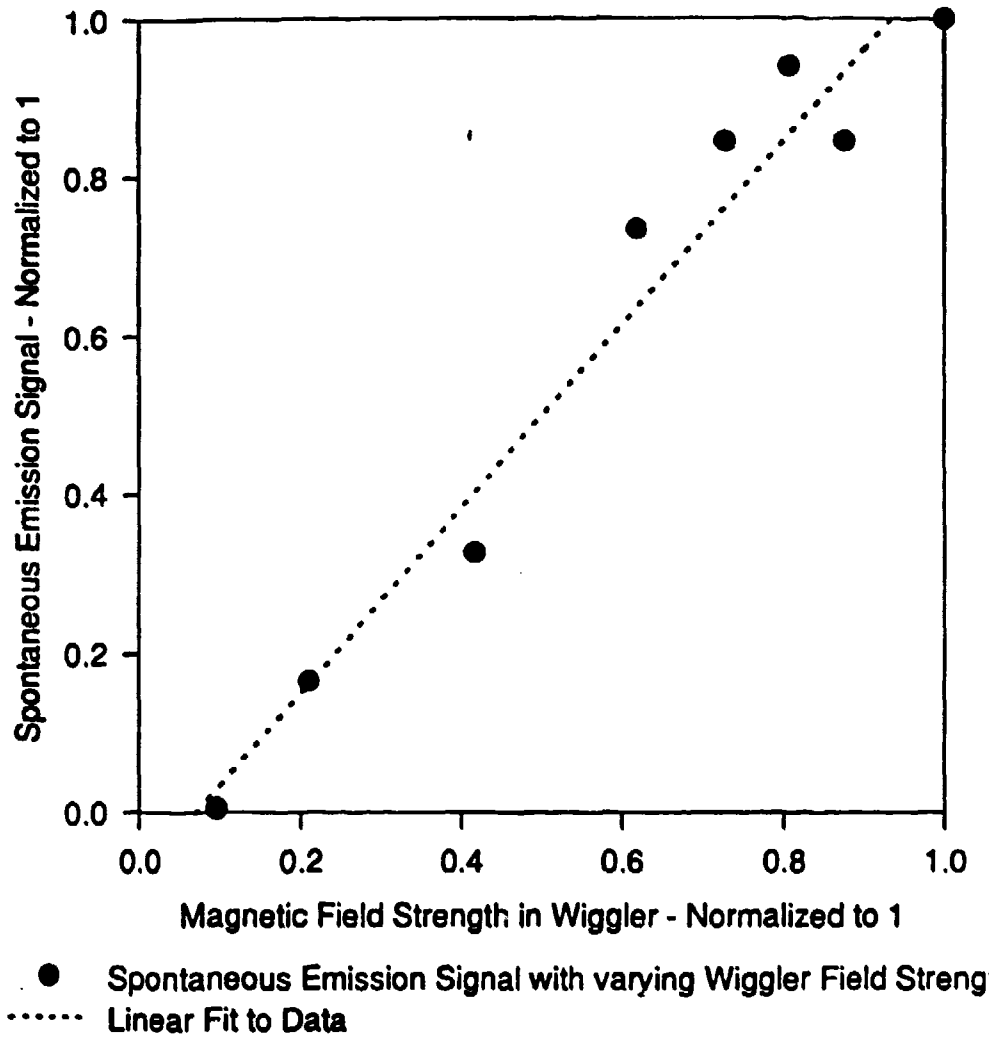

Figure 4 *Measured spontaneous emission signal at various wavelengths. Data taken with an electron beam energy of 40.86 MeV.*

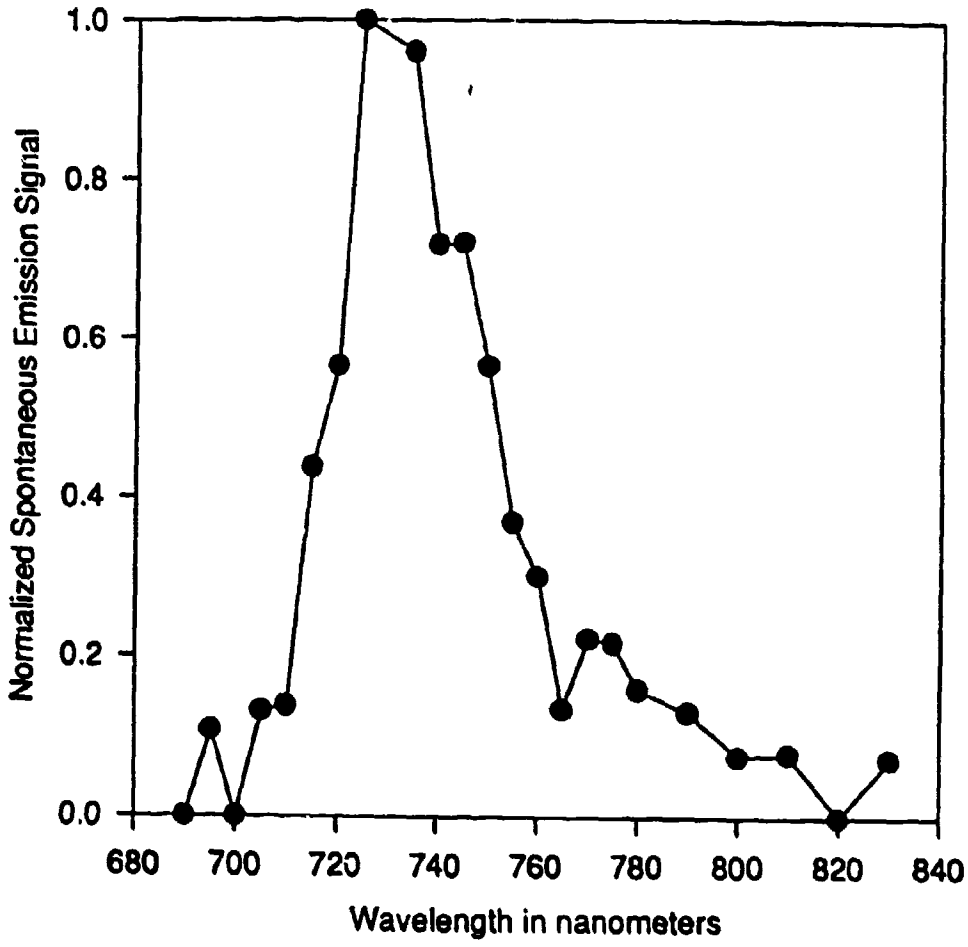

APPENDIX

A 70-PERIOD HIGH-PRECISION MICROWIGGLER FOR FREE ELECTRON LASERS

R.Stoner* and G. Bekefi
Department of Physics and Research Laboratory of Electronics
Massachusetts Institute of Technology
Cambridge, MA 02139

ABSTRACT

We have designed, constructed, and operated a 70-period microwiggler for free electrons lasers (FELs). The device is a pulsed ferromagnetic-core electromagnet with a period of 8.8 mm, which generates an on-axis peak magnetic field of 4.2 kG. The pulses, of 0.5 msec duration, are generated at a rate of 0.5 Hz. Each field peak is independently tunable. We employed a novel tuning regimen to reduce the RMS spread in the peak amplitudes to 0.12%, the lowest value thus far attained in a sub-cm-period periodic magnetic field.

* Present address: Smithsonian Astrophysical Observatory, Cambridge, MA 02138

1. Introduction

Size and cost reduction of visible and UV wavelength FEL systems is necessary if they are to become practical radiation sources. The use of a short-period (1-10 mm) microwiggler magnet permits higher frequency radiation to be generated with a device which is more compact than one employing wigglers of the usual period (typically 3-10 cm).

Microwiggler design and construction pose very serious engineering challenges. Mechanical tolerances of a given value become increasingly large in the fractional sense as the size scale is reduced, leading to correspondingly increased fractional field errors. Also, wiggler field strength falls off exponentially as the ratio of the separation between wiggler halves (the "gap") to the wiggler period. Therefore, maintaining a gap adequate to pass an electron beam (a few mm) while reducing the wiggler period results in significant field magnitude reduction unless corrective measures are taken. In spite of these difficulties, numerous groups have investigated short-period wigglers. A variety of techniques have been proposed and studied, some of which are: samarium-cobalt permanent magnet grooved slabs [1], ferromagnetic core stacks with interleaved copper sheets [2], high current pulsed-wire designs [3], electromagnet helical microwigglers [4, 5], staggered ferromagnetic core arrays immersed in a solenoidal field [6], superconducting ferromagnetic core designs [7], and hybrid samarium cobalt and iron microwigglers [8]. A common characteristic of most of these approaches is to control and minimize field errors by means of precise fabrication while dealing with steering errors (imparting of net transverse momentum to an electron beam) and deflection (imparting a net transverse displacement to an electron beam) with internal or external trim coils (note: Tecimer and Elias [8] used poleface shim tuning). These measures, while sucessfully employed in full-sized wigglers, have met with varying degrees of success in most of the above mentioned

designs, yielding errors of order several percent RMS spread in the amplitudes of the wiggler field peaks, as well as uncompensated end effects (notable exceptions being Benzvi *et. al.* [7], having attained field errors of order 0.28%, and Tecimer and Elias [8] having achieved 0.2%: see Table 1).

In contrast, we have constructed a 70-period planar microwiggler, having period 8.8 mm, which employs extensive tuning to accomplish field error reduction. Each half-period is independently adjustable, permitting great control over the amplitude profile. Also, we have developed a coil/ferrocore geometry permitting pulsed operation at high peak field amplitudes (4.2 kG) at experimentally useful repetition rates (>1/2 Hz). The design is an outgrowth of our earlier work [9]. We used amplitude tuning to produce a 70-period microwiggler with 0.12% RMS spread in the peak amplitudes, the lowest value we are aware of in a sub-cm-period wiggler.

This paper describes the construction of the microwiggler, as well as the magnetic field measurements which demonstrate its high field precision. We also describe the method employed for achieving efficient and accurate adjustment of the 140 degrees of freedom afforded by the extensive tunability of the microwiggler. In our conclusions, we estimate the performance limits of our design.

Section 2 describes the construction of the microwiggler. Field measurements are presented in Section 3. Section 4 describes the method employed to tune the microwiggler. Conclusions are presented in Section 5.

2. Construction of the microwiggler

The microwiggler is a 70-period device with an 8.8 mm period and a 4.2 mm gap, consisting of 280 electromagnets held by a precisely formed aluminum matrix. Figure 1 illustrates the geometry of the microwiggler (and the coordinate axes used to describe the wiggler geometry); Figure 2 is a photograph of the microwiggler. Each electromagnet is formed from wire wound on a core consisting of six Microsil laminations of dimension 12.7 x 25.4 x 0.35 mm (29 gauge). Microsil was chosen in favor of more exotic materials (like vanadium permendur) because of its extremely low cost and ready availability, and its very small hysteresis and remnant fields. A very high degree of uniformity was achieved in the thickness of the laminated cores: the thicknesses of all 280 cores lay within a range between 2.101-2.106 mm. This precision was attained by sorting 2000 individual laminates according to thickness, and then judiciously selecting sets of laminates having the proper total thickness. Figure 3 shows an individual electromagnet, each of which was hand-wound with 50 turns of 32 AWG Formex wire.

The individual coils are placed in two aluminum holder pieces to form a wiggler configuration. Each holder consists of a bar fashioned from aluminum jig-plate stock with 140 slots cut perpendicular to the longitudinal axis of the bar: each slot accomodates an individual electromagnet. The two aluminum holder pieces lie on each side of the wiggler gap, and are aligned by a pin-and-socket arrangement at each end of the holders.

The coil holders were manufactured with considerable precision. Neither the width nor the cumulative (axial) positional error of any of the 140 coil holder slots in each holder exceeds 0.01 mm. The gap separation is determined by the aluminum holders. Figure 4 is a section drawing showing the assembly of the wiggler halves, drift tube, etc. The rectangular electron drift tube consists of a 75 cm length of 0.25 mm-wall-thickness

stainless steel K_a band waveguide, with stainless mini-CONFLAT flanges braised onto each end. Longitudinal slots cut into each end of the magnet holders secure the drift tube position. The transverse position of the drift tube is also very well-fixed by the polefaces; this is crucial because the pickup coil probe for magnetic field measurements takes its position via a slip fit inside the drift tube. Measurement of the relative height of each of the 280 polefaces shows that the highest polefaces are randomly distributed through the wiggler, and that they fix the transverse (y) position of the drift tube to better than 20 microns. Drift tube wall thickness variations thus yield as much (or more) drift tube position error as poleface height variations.

Two electromagnets facing across-gap from one another comprise a half-period, and are connected in parallel to ground and to the current source through a tuning resistor. Figure 5 illustrates this arrangement schematically. The wiggler circuit consists of 140 half-period pairs, connected in parallel to the current source. Tuning is accomplished by means of variable resistors. They consist of 22 AWG manganin wires, the lengths of which are varied to adjust their resistances. Tuning of the microwiggler therefore consisted of adjusting the value of 140 resistors in a resistive current divider network. Care was taken to energize the microwiggler with pulses of long duration (880 μsec) compared to the (L/R) time of the microwiggler (about 60 μsec), to ensure that the impedance of the various half-period circuit elements remained primarily resistive.

2. Field measurements

The measured peak amplitudes of our microwiggler are plotted in Fig. 6, as a function of peak number, before and after tuning. Two peaks at each end are tapered for minimal beam steering and deflection. A zero-steering POISSON model was generated, and the amplitudes obtained therefrom were tuned into the ends of the Microwiggler. For

these and all other measurements described in this section (the saturation data excepted), the microwiggler was operated at a repetition rate of 1/2 Hz, and energized with underdamped half-sine waves of half-period 880 μsec. The mean field amplitude was 4.2 kG.

The RMS spread in the peak amplitudes, excluding the ends of the magnet, is 0.12%. This fact is by itself inadequate to establish that the RMS spread in the pole integrals (i.e., the areas under the B_z *vs.* z curve of each half-period) is small, however, and the RMS spread in the pole integrals is a preferred figure of merit for wiggler field uniformity. In lieu of a detailed field profile measurement (which our measurement system could not produce with adequate precision to assess the field uniformity), we measured the position of each peak, in addition to its amplitude. Figure 7 is a plot of the position difference of each peak from perfectly equidistant spacing. The RMS spread in the position errors is 9 μm, or 0.1% of the period. We have found that the correlation function of the position and amplitude error profiles show no correlation between the position and amplitude errors, so that we can estimate the RMS spread of the pole integral profile to be $\sqrt{(0.0012)^2 + (0.001)^2} = 0.16\%$.

Additional measurements are required to ensure that our peak amplitude and position measurements are not significantly affected by possible systematic errors. One such error could conceivably arise from the fact that the half-periods are wired in parallel (Fig. 5): variations in inductive impedances among the half-periods could cause variations in their fields' time dependence. In particular, the effective inductance of the half-periods at the ends is less than that of half-periods in the body, because of the reduced mutual inductance of the two end half-periods. Figure 8 is a plot of the relative times, for half-periods near each end of the magnet, at which the magnetic field reached its peak value. A

measureable shift occurred at the ends, but only amounts to a part in 10^3 amplitude reduction of the end half-periods. The random variations in the time-to-peak of the half-periods in the magnet body can be shown to result in an RMS field error less than a part in 10^4. Thus, the effect of time-to-peak variations is completely negligible.

Another concern is whether the pickup coil probe is actually guided along the axis of the wiggler. Systematic errors could result were the probe not moving parallel to the wiggler axis during the peak amplitude measurements. We addressed this concern by using a probe sensing B_z (rather than B_y) (see Fig. 1), to measure the position of the field's cross-gap minimum. In an ideal magnet with such a probe perfectly centered on the z-axis, no signal would ever be detected. In the real magnet, however, the magnetic field center and the pickup coil center do not exactly coincide, so that some axial field component of the wiggler field was sensed by the pickup coil. The signal was directly proportional to the separation between the pickup coil center and the magnetic center. To obtain maximum signal from the axial probe, it was positioned near nulls of the B_y magnetic field component; the axial component B_z is a maximum at those points. Measurements were taken at each of the 139 transverse field component nulls. Figure 9 shows plots of the analyzed data and its Fourier transform. Fourier components at spatial frequencies of zero and $1/\lambda_w$ were removed from these data, since they were due to either a constant offset of the coil from the mean magnetic center, or a spurious pickup due to the coil being slightly tilted and thus sensing some magnetic field component B_y.

The axial probe measurements show an RMS deviation of the magnetic field center from the pickup coil center of less than 17 microns. This value is conservative, in that it includes contributions of Fourier peaks which are possibly due to translator error. The field amplitude RMS variation due to this magnetic center position variation, along the pickup coil center's axis of travel, is of order

$$\delta B_{y,\mathrm{RMS}} \approx B_w \cdot \left(\frac{1}{2}(k_w \delta y_{\mathrm{RMS}})^2\right) < 1 \times 10^{-4} \cdot B_w \qquad (1)$$

where $k_w = 2\pi/\lambda_w$, and λ_w is the wiggler period; δy_{RMS} is the RMS deviation of the cross-gap field minimum from the wiggler axis; and B_w is the wiggler field amplitude. This variance is negligibly small in comparison to the measured RMS spread in the peak amplitudes of 0.12%. Thus, the magnetic center position variation need not be considered in the tuning of the transverse field amplitude. It should be emphasized that what was measured are the differences in position between the magnetic center and the axis of the magnet bore. There is no way to know from these data whether the bore axis is straight or not, though the use of strong, precisely-machined 1 1/2"-thick aluminum stiffener elements to enforce straightness of the magnet holders offers reassurance that the holders are straight to a precision of tens of microns or better. Moreover, the distances of each of the 280 polefaces from a reference plane (the flat backs of the holders) were measured to a precision of ±3 μm. These measurements determined the cross-sectional area into which the drift tube is confined. Its position is fixed to within about 10 μm in the *y*-direction. Mechanical tolerances thus ensure that the measurement probe was being borne parallel the mechanical axis of the magnet, and that the mechanical axis is straight; the data of Fig. 9 show that there is no significant variation of the magnetic axis from the mechanical axis. The cross-gap minima positions are thus very close to colinear.

A portion of a detailed scan of the wiggler magnetic field profile is shown in Fig. 10, along with a Fourier transform of the entire profile (excluding the periods at each end). We find that the power spectral density of the second and fourth harmonics are below the noise level; the third harmonic is down from the fundamental by a factor of about 2.3×10^{-5}. This is a very small value, which is advantageous for use in a short-wavelength FEL oscillator because higher field harmonics cause very short-wavelength incoherent emission

which can damage optical coatings of resonator mirrors. The measured fifth harmonic is just above the noise level, at around 6×10^{-6}, which is also small.

The measured magnetic field vs. current profile of the microwiggler is depicted in Fig. 11. This curve was used to select the value of the operating peak field (4.2 kG). These measurements were made with long (16 msec) current pulses injected into a 20-period subsection, which permitted the use of a Hall probe gaussmeter. The wiggler gap was 4.4 mm when these measurements were made. It subsequently became possible to reduce the gap to 4.2 mm (the present value), to boost the wiggler field. The fundamental component of the wiggler field depends on the wiggler gap G as

$$B \propto e^{-\frac{\pi}{\lambda_w} G} \qquad (2)$$

when G is a substantial fraction of the wiggler period λ_w. We estimate that the fields for a given current are about 4-6% larger with the present smaller gap than the measurements of Fig. 11. This estimate was confirmed via the integrated ($\dot{B}$) pickup coil signal, which indicated a peak magnetic field of (4.5 ± 0.3) kG.

3. Field measurement and tuning techniques

To attain a precision of 0.12% in the RMS spread of the field peak amplitudes, a very large number of measurements had to be made to reduce measurement error. A systematic approach to adjusting the 140 tuning resistors had also to be applied. The current energizing the wiggler needed to be constantly monitored and adjusted. Manual control by a human operator was impractical; consequently, we developed a computer-based system for performing field measurements, monitoring and regulating the microwiggler's operation, and computing resistor adjustments based on field measurement results. ($\dot{B}$) pickup coils sensed the wiggler magnetic field as well as that surrounding the

high current bus. The magnetic field pickup coil was of extent 1mm x 1mm x 5mm in the axial (z), cross-gap (y) and transverse (x) directions, respectively, and consisted of 8 turns of 32 AWG Formex copper wire wound in two layers on a rectangular G-10 core. The current pickup coil was in the Rogowski configuration. The signals were integrated using analog electronics and the integrated signals were digitized by a PC-based A/D board. The analog integrator circuits needed to be well-isolated from interference produced by the pulser. We chose this approach in favor of a Hall probe since the available Hall probe system lacked the bandwith to accurately capture the magnetic field pulse. Use of a DC measurement scheme in an attempt to overcome the bandwidth problem was impractical since the magnet operates in the saturated regime of the ferromagnetic cores (requiring very high current to reach). The computer extracted the peak values of the integrated wiggler field and current pulses and recorded them in memory, periodically writing accumulated sets of shot data to disk.

It should be emphasized that current stabilization was absolutely necessary for attaining a steady magnetic field amplitude. In the absence of active control, capacitor conditioning effects lead to current amplitude drifts of several percent over the course of a day's run; a drift of such magnitude is intolerable. The computer-controlled current stabilization eliminated the long-term drift, and resulted in an RMS spread in the current peaks over a day's run ($>2 \times 10^4$ shots) of less than 0.1%. Since the magnet operated in the saturated regime, this meant that the shot-to-shot jitter and the long-term drift in the magnetic field amplitude combined to less than 0.03%, an acceptable value. The resulting jitter/drift in the center frequency of FEL radiation wavelength resulting from the shot-to-shot field jitter is then of order 0.003%.

The tuning regimen viewed the magnetic field profile as a 140-component vector, the components of which were the amplitudes of the 140 field peaks. A stepper-motor-

driven translator pulled the ($\dot{B}$) pickup coil through the wiggler drift tube; a holder fitted to the drift tube supported the pickup coil, and attached to the translator via a length of stainless steel tubing. The pickup coil leads were brought out of the wiggler through the stainless steel tubing in twisted pair configuration. Grounded-shielded twisted-pair cable brought the signal to the analog integrator.

The magnetic field peaks were measured in sequence. The probe moved in steps of 0.25 mm; 5-7 data points were taken in the vicinity of each peak. Upon sensing a change in the spatial derivative of the field (as a function of axial position), the computer recognized that a peak had been found. It moved the probe one more step, took one more datum and moved the probe several millimeters to the vicinity just before the next peak: the polarity of the ($\dot{B}$) pickup coil probe connections were then reversed (via a relay network) so that the sign of the electronic pulse presented to the analog integrator remained unchanged as the polarity of the field changed.

After getting data for a peak, the computer performed a least-squares fit to a parabola to extract the peak value (a parabola was used because it is an adequate model to which the data can be rapidly fit); the result was recorded in memory. The sequence of 140 peak measurements was repeated 5-6 times and the results were averaged. Since each sequence of 140 measurements provided an independent measurement of each peak, we also computed the standard deviation in the mean of the measurements to obtain an estimate of the statistical uncertainty in the measurement of each peak. The typical uncertainty was 0.035%.

Of course, systematic errors must also be controlled. Extreme care was taken in the construction of the pickup coil probes in order to avoid spurious pickup by the leads coming out of the magnet bore. The pickup coil and the leads were formed of a single

piece of 32 AWG Formex wire. This was necessary because the use of solder junctions located at the pickup coil to attach the pickup coil to the output leads resulted in an inadvertent extra pickup loop which acquired significant spurious signal. The output leads were brought out in a twisted-pair configuration of 1200 turns placed on the 60-cm leads; longer pitches in the twist were found to result in undesired pickup from the leads. Moreover, the twisted pair ($\dot{B}$) signal cable (from wiggler to integration electronics/computer) had to be carefully routed away from the pulser to eliminate a false indicated dipole field component. Care was also taken to avoid creating an inadvertent pickup loop at the signal cable-pickup probe leads junction, which when made too large could sense the stray fields from the pulsed power supply. Measurements using various probe orientations and lead connections were compared in order to identify and eliminate these problems.

Having precisely measured the field profile, it remains to apply corrections to reduce the errors. This requires advance determination of a reasonable "target" field profile, and careful characterization of the effects of making adjustments to the tuning resistors. Determining an experimentally useful target profile is not trivial: since the field peaks change shape at the ends of the wiggler, one must relate the measured peak amplitude to the total integral of the field in the end peaks. In doing so, it is necessary to account for the fact that the ($\dot{B}$) pickup probe has both axial and transverse extent, and so the measured field at a given point is really the value averaged over the extent of the probe. We took the approach of tuning a "virtual wiggler" in the POISSON codes, using a target profile in which the integrals of the first and last half-periods (taken on axis) of the wiggler were taken to be 1/2 that of half-periods in the body of the magnet (the techniques used in the virtual wiggler tuning were identical to those outlined below for the actual magnet). This profile produces zero net steering of an on-axis electron beam. We then calculated what profile our pickup probe would measure from the virtual wiggler's field by

computing averages over the pickup coil extent for a dense sample of coil positions. This profile was then analyzed to compute the amplitudes of the peaks that would be measured from a zero-steering wiggler field. We found that the first two peaks' measured amplitudes must be reduced in comparison to those of the body of the wiggler, in the ratio 0.37 : 0.88: 1.00.

Having found a target tuning profile, the effects of tuning resistor adjustment must be systematically probed. The known set of necessary field amplitude changes must be translated into a set of resistor adjustments via a matrix whose components are defined by

$$\left(\frac{\partial B_i}{\partial R_j}\right) = \{\text{change in } i^{th} \text{ peak amplitude due to change in } j^{th} \text{resistor}\} \qquad (3)$$

This is a (140 x 140)-component matrix; all of its components are measurable in principle, but in practice a judiciously chosen subset must be selected. We measured a (11 x 11) matrix using the first eleven peaks of the wiggler, in order to capture the ends' behavior while proceeding far enough into the wiggler bulk to accurately characterize it. The measured matrix was then extended to full dimension by assuming symmetry about wiggler center and neglecting effects of resistor adjustments more than 3 peaks away from a given resistor. A change in the field profile vector ($\Delta\vec{B}$) is then produced by a resistance adjustment vector ($\Delta\vec{R}$) according to the matrix equation

$$\Delta\vec{B} = \frac{\partial\vec{B}}{\partial\vec{R}} \cdot \Delta\vec{R} \qquad (4)$$

where the desired ($\Delta\vec{R}$) can be computed from the measured ($\Delta\vec{B}$) field differences from the target profile and the measured ($\partial\vec{B} / \partial\vec{R}$) response matrix. This procedure amounts to a Taylor expansion to linear order of the magnetic field amplitude profile vector as a function of the tuning resistor values, about the initial value of the field amplitude profile

vector (typical tuning resistances are roughly 5-10% of the coil resistances). Of course, our use of ferrocore electromagnets in the saturated regime ensures that, for sufficiently large changes in the tuning resistors, nonlinear variations in the field would be produced. Nevertheless, iterative application of the procedure rapidly converged to the measurement precision limit. Only 3 iterations were required to reduce the RMS spread in the peak amplitudes from the untuned value of 4% to a value of 0.12%.

4. Comments and conclusions

A tunable electromagnet wiggler was used in the first free electron laser [11], so that wiggler tunability is by no means a new concept. However, ours is the first device of which we am aware in which many tens of degrees of freedom have been systematically and efficiently exploited. In only a handful of iterations, our novel tuning algorithm produced a uniform-amplitude field profile (with end-tapering) with an RMS spread in the peak amplitudes of 0.12%, the most precise sub-cm-period wiggler field to date. Table 1 compares our microwiggler with some other recently-reported short-period wigglers.

Reduction in the RMS spread of the pole integrals to the 0.05% level is readily achievable in our device. This would be comparable to the world's most uniform periodic magnetic field, but at 1/3 the wiggler period- a formidible achievement. An improvement in the uniformity of the untuned profile would be required in order to reduce the magnitude of certain of the tuning resistances, but such an improvement could be made using a technique employed in samarium cobalt wigglers [12]: the individual electromagnet coils could each be tested and sorted according to their field strengths produced by a standard input current. Coils with field strengths outside a specified range could be re-wound. The coils would then be re-installed in order of increasing or decreasing strength, according to whether or not a particular order would be preferred to

implement a possible field tapering scheme. In this fashion, random error is transformed into systematic variation and the total spread in the peak fields' values is reduced. Also, we are at this writing in the process of converting to a pole integral measurement scheme using our present electronics, and anticipate similar precision to the peak amplitude measurements will be attained (0.035%), which is adequate to enable attainment of 0.05% RMS spread in the pole integral profile.

In conclusion, we have constructed and operated a ferromagnetic-core based electromagnet wiggler having 70 periods of 8.8 mm and a gap of 4.2 mm, producing an on-axis wiggler field of 4.2 kG in 0.5 msec pulses at a repetition rate of 0.5 Hz. We claim that the field produced has the smallest RMS spread in the peak amplitudes, 0.12%, and the smallest spread in the pole integrals, 0.18%, of any sub-cm-period wiggler yet reported. We have performed an extensive battery of measurements to support this claim. Our microwiggler is presently being used in a visible- and UV-wavelength FEL oscillator experiment at the Accelerator Test Facility, Brookhaven National Laboratory.

5. Acknowledgements

This work was supported by the Office of Naval Research. Thanks are due to J. Blastos, I. Mastovsky, and D. Sisson for their assistance in the construction and field measurement effort. We are also grateful to I. Ben-zvi and X. Wang at the Accelerator Test Facility, for generous facility access and for useful conversations.

References

1. "Micro-Undulator Fields," I. Kimel and R. Elias, *Nucl. Instr. and Meth.*, A296, 611 (1990). "Micro-Undulator FELs," G. Ramian, L. Elias and I. Kimal, *Nucl. Instr. and Meth.*, A205, 125 (1986).

2. "Propagation of Wiggler Focused Relativistic Sheet Electron Beams," J.H. Booske, W. W. Destler, Z. Segalov, D.J. Radack, E.T. Rosenbury, J. Rodgers, T.M. Antonsen, Jr., V. L. Granatstein, and I.D. Mayergoyz, *J. Appl. Phys.*, 64 (1), 6 (1988).

3. "High-Field Pulsed Microwigglers," R.W. Warren, D.W. Feldman, D. Preston, *Nucl. Instr. and Meth.*, A296, 558 (1990).

4. "Development of an Electromagnetic Helical Microwiggler," N. Ohigashi, K. Mima, Y. Tsunawaki, S. Ishii, N. Ikeda, K. Imasaki, M. Fujita, S. Kuruma, A. Murai, C. Yamanaka, S. Nakai, *Nucl. Inst. and Meth.*, A341, 426 (1994).

5. "Design of a High-Field Taperable Helical Wiggler," J. Vetrovec, *Nucl. Instr. and Meth.*, A296, 563 (1990).

6. "Performance Characterization of a Far-Infrared, Staggered Wiggler," Y.C. Huang, H.C. Wang, R.H. Pantell, J. Feinstein, J. Harris, *Nucl. Instr. and Meth.*, A341, 431 (1994).

7. "Performance of a Superconducting, High Field Subcentimeter Undulator," I. Ben-Zvi, R. Fernow, J. Gallardo, G. Ingold, W. Sampson, M. Woodle, *Nucl. Instr. and Meth.*, A318, 781 (1992).

8. "Hybrid Microundulator Designs for the Creol Compact CW-FEL," M. Tecimer and L.R. Elias, *Nucl. Inst. Meth.* A341, ABS 126 (1994).

9. "A Planar Electromagnet Microwiggler for Free Electron Lasers," R. Stoner, S.-C. Chien, G. Bekefi, *IEEE Trans. on Plas. Sci.*, 18 (3), 387 (1990).

10. "Proposed UV-FEL User Facility at BNL," I. Ben-Zvi, L.F. DiMauro, S. Krinsky, M.-G. White, L.H. Yu, K. Batchelor, A. Friedman, A.S. Fisher, H. Halama, G. Ingold, E.D. Johnson, S. Kramer, J.T. Rogers, L. Solomon, J. Wachtel, and X. Zhang, *Nucl. Instr. and Meth.*, A318, 201 (1992).

11. "The Ubitron, A High-Power Traveling-Wave Tube Based on a Periodic Beam Interaction in Unloaded Waveguide," R.M. Phillips, *I.R.E. Trans. Elec. Dev.*, 7, 231 (1960).

12. "FEL Performance with Pure Permanent-Magnet Undulators Having Optimized Ordering," R.A. Cover, B.L. Bobbs, G. Rakoswky, M.M. Johnson, S.P. Mills, *Nucl. Inst. and Meth.*, A296, 603 (1990).

13. "Lasing in Visible and Ultraviolet Regions in an Optical Klystron Installed on the VEPP-3 Storage Ring," I.B. Drobyazko, G.N. Kulipanov, V.N. Litvinenko, I.V. Pinayev, V.M. Popik, I.G. Silvestrov, A.N. Skrinsky, A.S. Sokolov, N.A. Vinokurov, *Nucl. Instr. and Meth.*, A282, 424 (1989).

Figure Captions

Figure 1. Microwiggler geometry. Coordinate axes are shown. Current flow in adjacent coils have opposite handedness, while current flow in cross-gap pairs have the same handedness. Parameter values: λ_w= 8.8 mm, G = 4.2 mm, T = 3.1 mm, W = 2.3 mm. Note that the gap shown is larger than in the actual design.

FIGURE 2. The microwiggler. The high-current busswork (top) delivers 12 kA in 0.5 msec pulses, which is distributed by the current distribution network. Current is delivered to each of the 280 coils by way of a 22 AWG twisted pair.

FIGURE 3. An individual electromagnet. The side view on the left shows a core without windings, to better illustrate the structure of the core/endpiece assembly. The mylar sheet is indispensible: in tests, fully half of coils made without it were electrically shorted to the core, a catastrophic failure rate.

FIGURE 4. Wiggler assembly section drawings. The top view shows how the holders, coils, and drift tube are assembled. The bottom view illustrates the installation of the coils into the aluminum holders.

FIGURE 5. Schematic of the pulsed power supply for the microwiggler.

FIGURE 6. Untuned (upper plot) and tuned (lower plot) peak amplitude profiles of the Microwiggler. The ranges and scales of the two plots are identical; very clearly, tuning has greatly reduced peak amplitude variations. The tuned profile also shows the tapering of the end peaks.

FIGURE 7. The measured positions of the peaks, with respect to their ideal, equidistant separations. The Fourier transform power spectral peaks indicated in the bottom plot are peaks due to translator error.

FIGURE 8. Time to peak of the magnetic field at half-periods at each end of the Microwiggler. The field at the end half-periods reaches a peak about 20 μsec later than the field at peaks in the magnet body. In both plots the measurements are connected by lines, to guide the eye.

FIGURE 9. The position of the wiggler magnetic field *y*-minimum (magnetic center) as a function of axial position *z* (top plot), and the Fourier power spectrum of the magnetic center position profile. We suspect two peaks in the power spectrum to be due to translator error, they are indicated in the bottom plot.

FIGURE 10. Detailed measurement of the axial field profile, and its Fourier transform power spectrum. The top plot is a portion of the profile measurements near the end of the magnet. The bottom plot is the power spectrum of the central 66 periods. The first, third, and fifth harmonics are indicated: harmonics beyond the fifth are obscured by noise.

FIGURE 11. Microwiggler field as a function of input current. These measurements were obtained with a Hall probe gaussmeter with the wiggler gap G = 4.4 mm. The gap was subsequently reduced to 4.2 mm to increase the field strength: the field at the operating current of 45 amperes per coil is now about 4.2 kG.

Table 1: Comparison of some short-period wigglers

GROUP	TECHNOLOGY AND STATUS	#PER.	λ_w/mm G/mm	B_w/kG	PEAK RMS ERROR	POLE INT. ERROR
Stoner *et. al.* MIT	Pulsed ferrocore electromagnet; operational	70	8.8/4.2	4.2	0.12%	0.18%
Huang *et. al.* Stanford	Staggered ferro-core array in solenoid; test	50	10.0/2.0	10.8	1.2%	Not reported
Warren and Fortgang LANL	Permanent magnet; operational	73	13.6/1.5	6.5	0.3%	Not reported
Tecimer and Elias CREOL	Hybrid; test	62	8/Not reported	1.0	0.2%	0.6%
Ben-zvi *et. al.* BNL	Superconducting ferrocore electro-magnet; test	20	8.8/4.4	>5.5	0.29%	0.36%

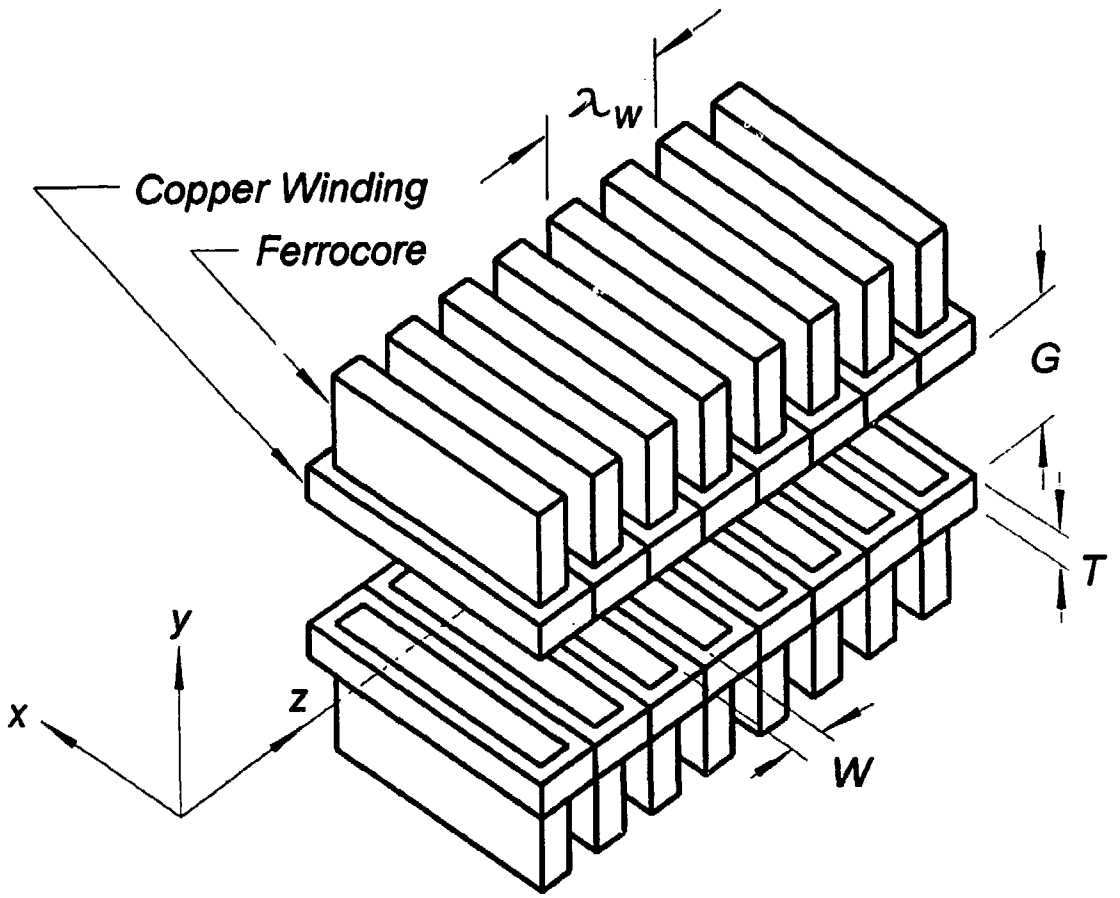

Figure 1. Stoner and Bekefi

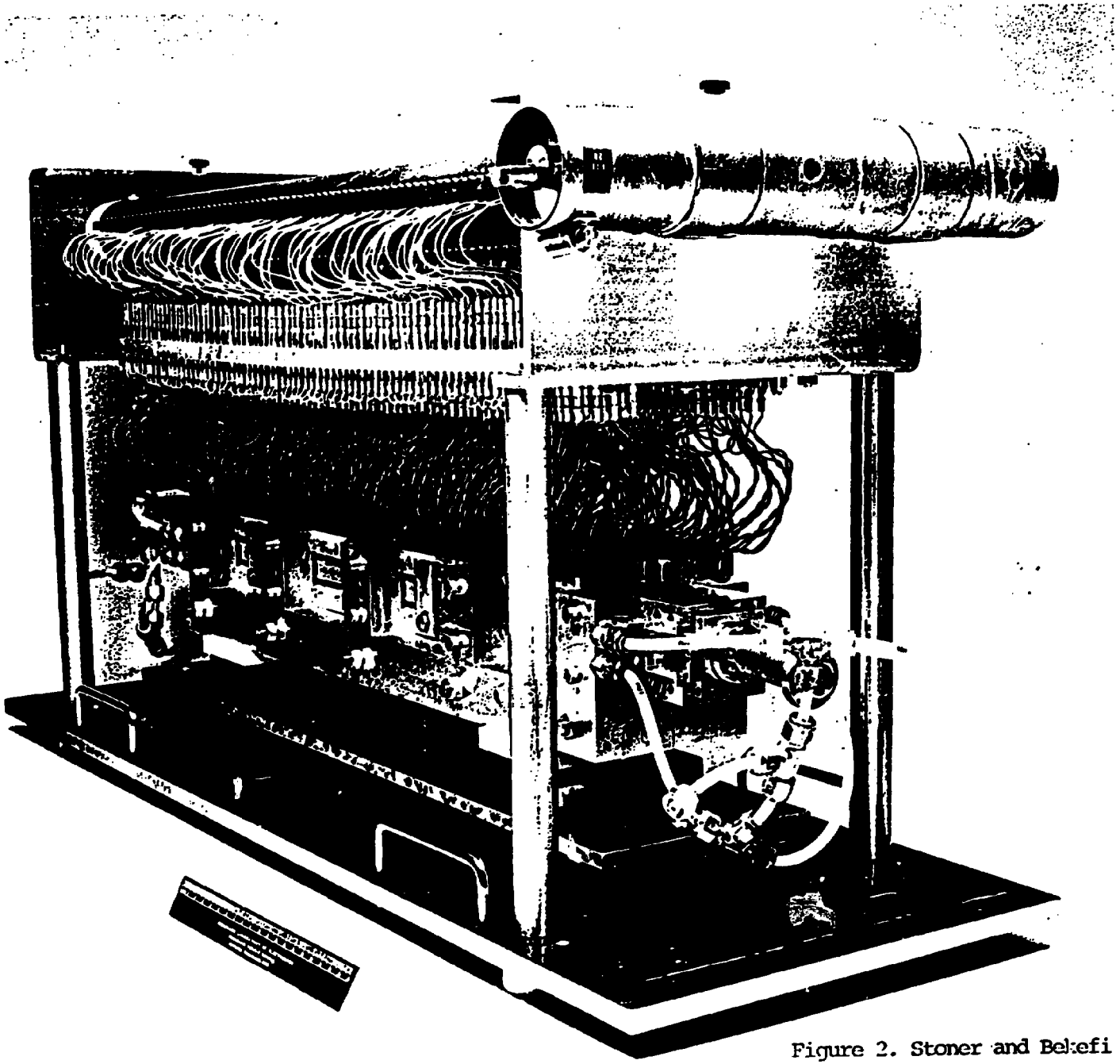

Figure 2. Stoner and Belzefi

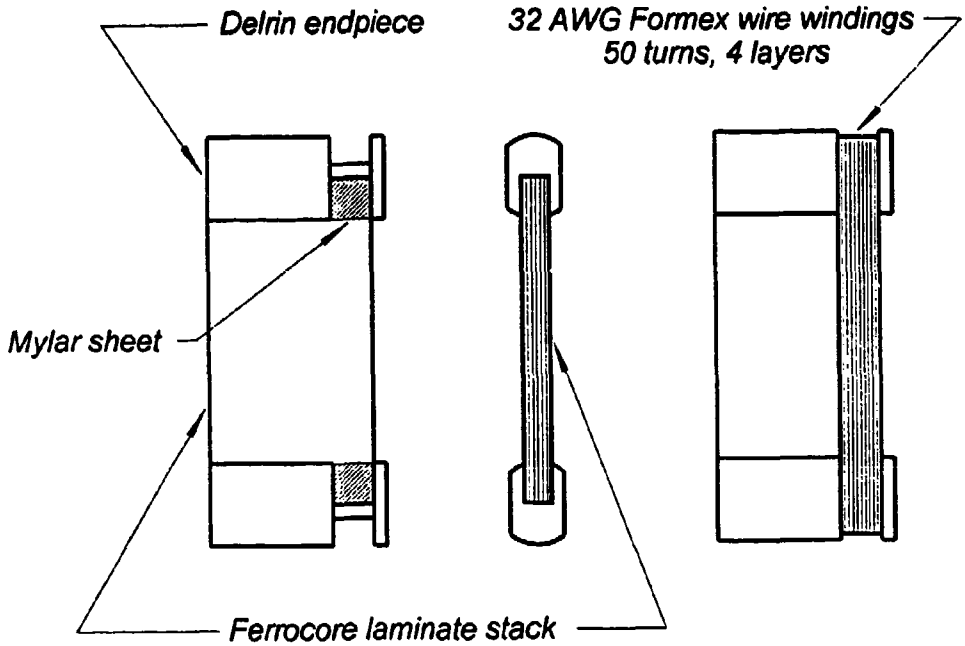

Figure 3. Stoner and Bekefi

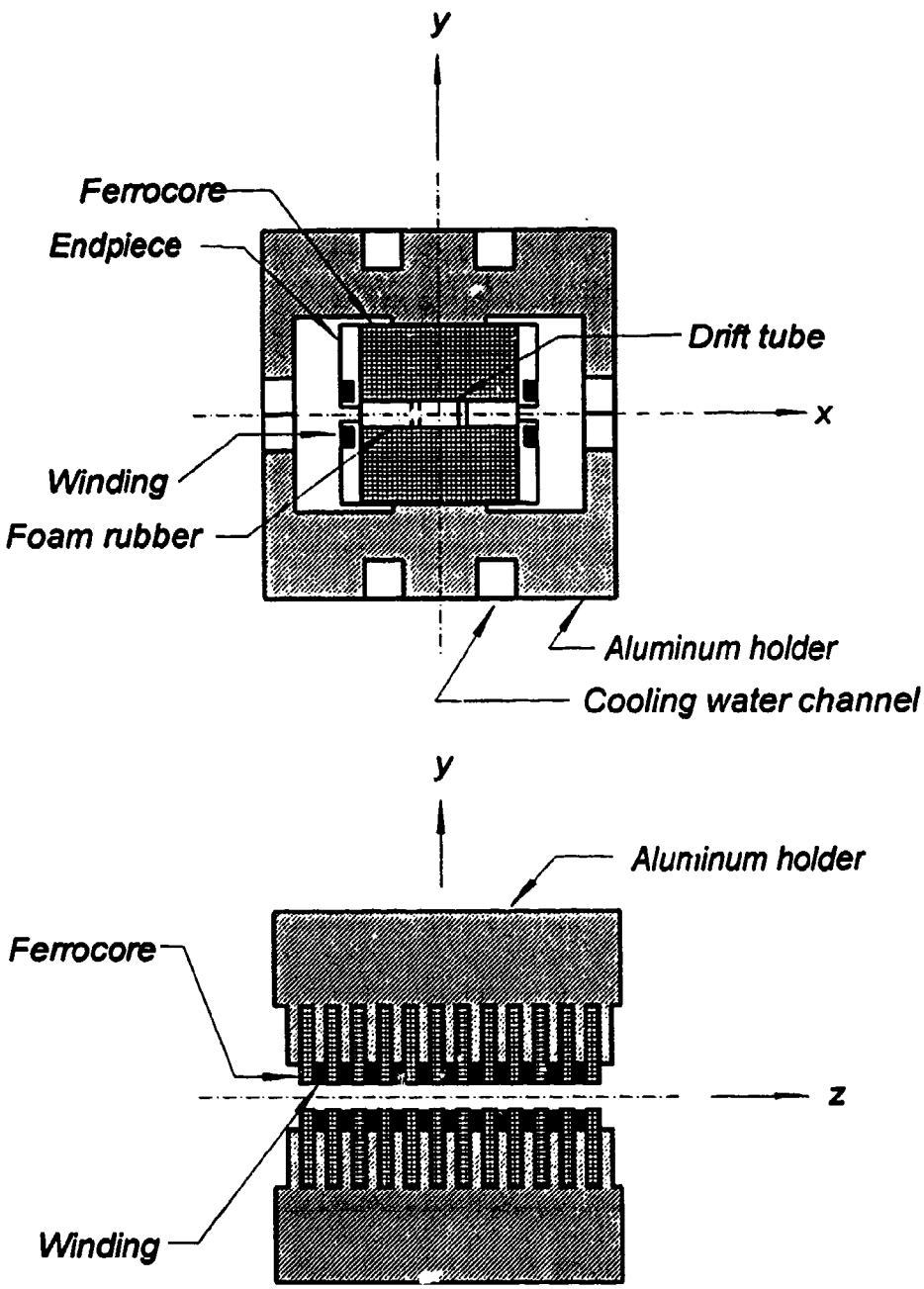

Figure 4. Stoner and Bekefi

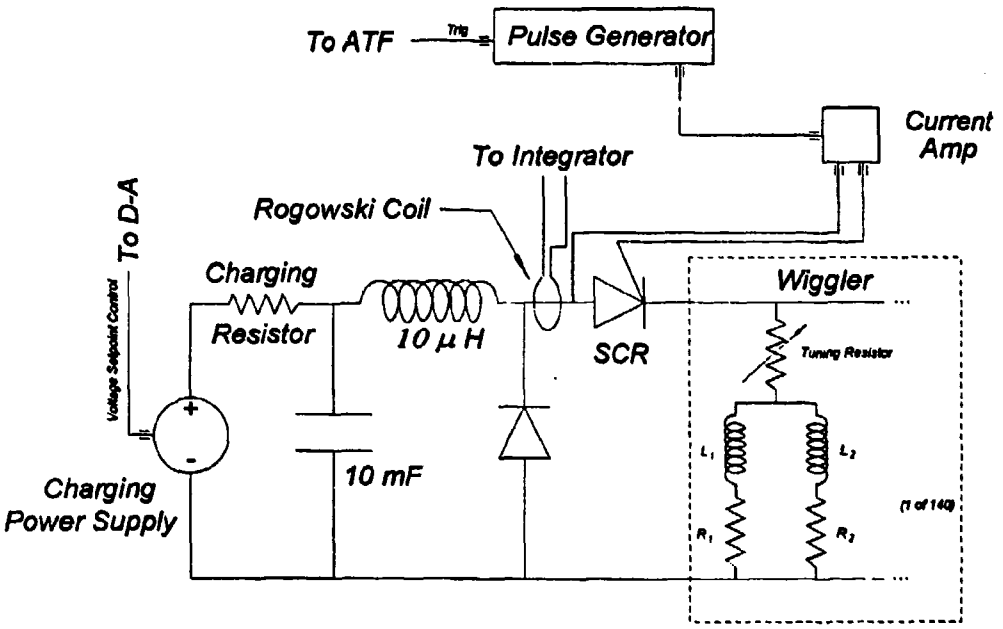

Figure 5. Stoner and Bekefi

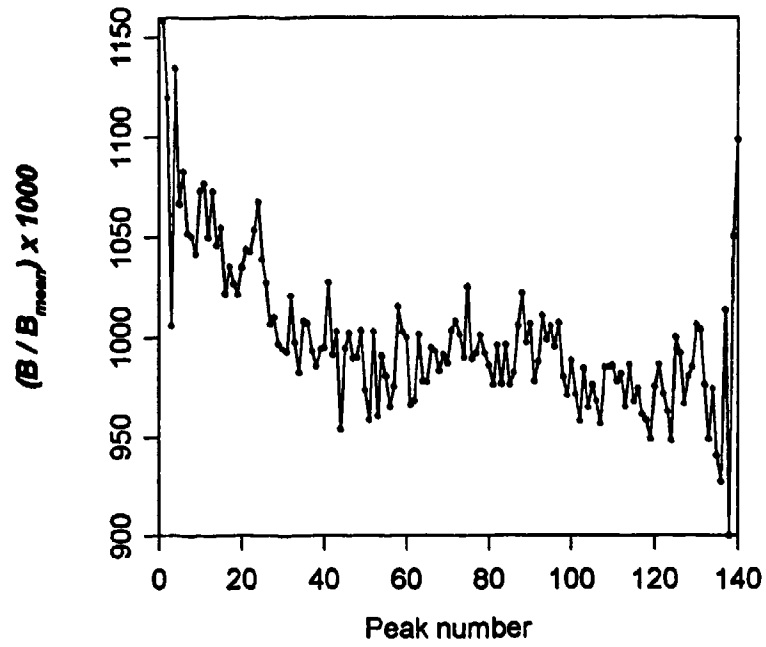

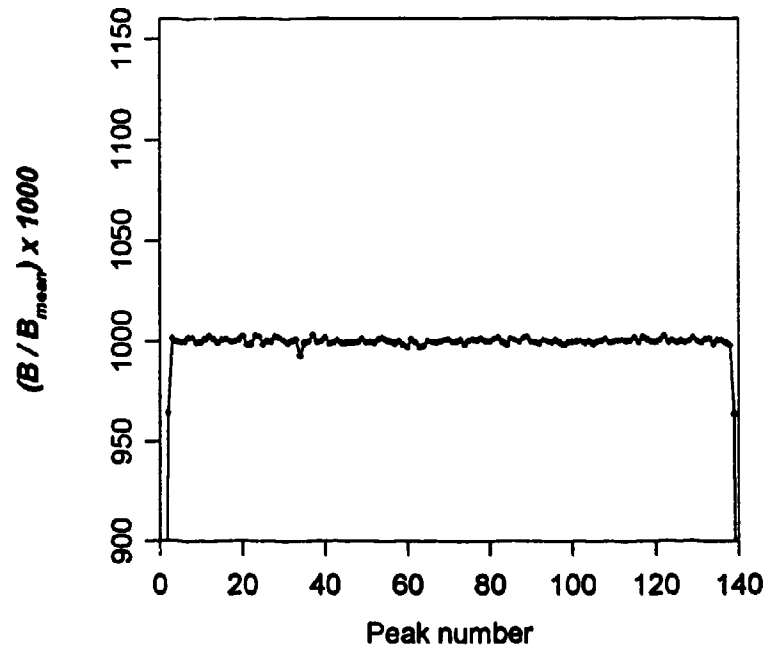

Figure 6. Stoner and Bekefi

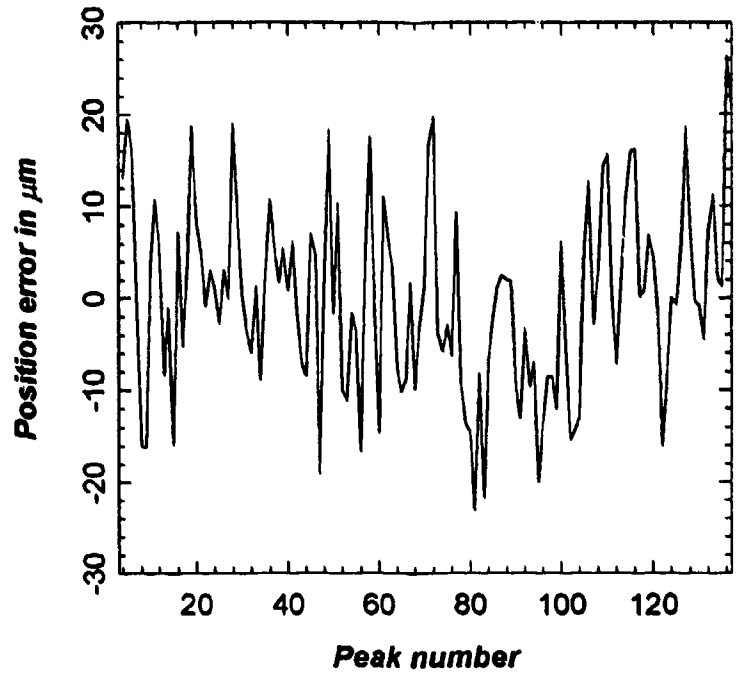

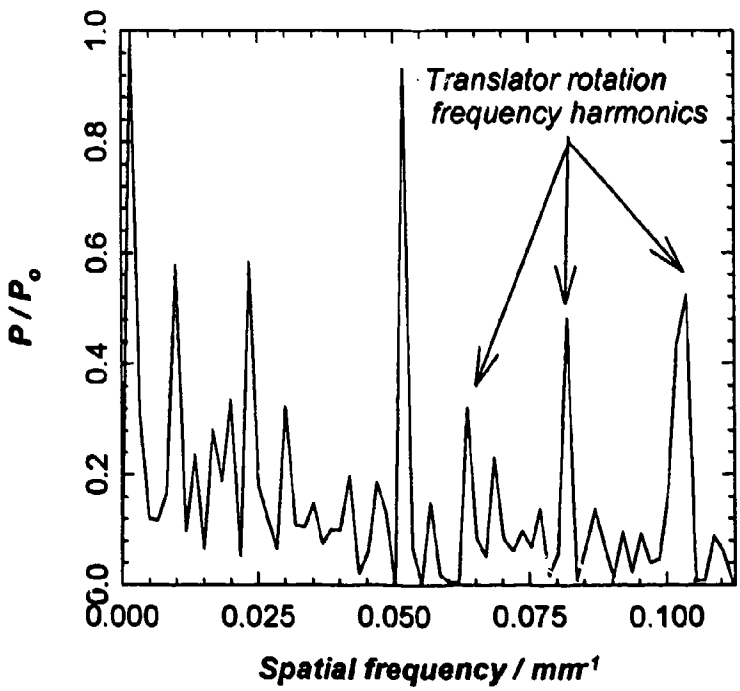

Figure 7. Stoner and Bekefi

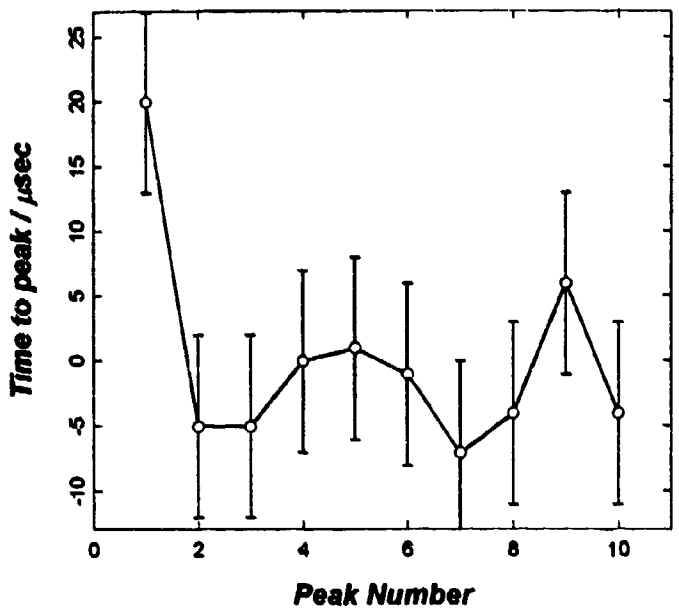

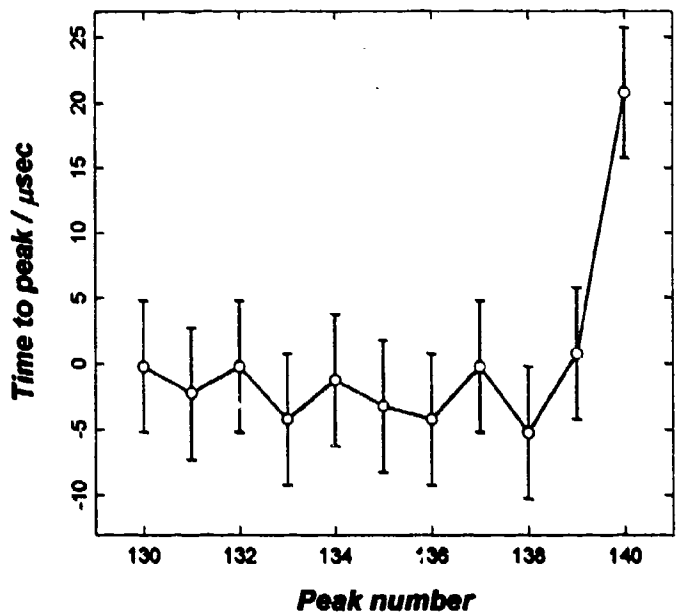

Figure 8. Stoner and Bekefi

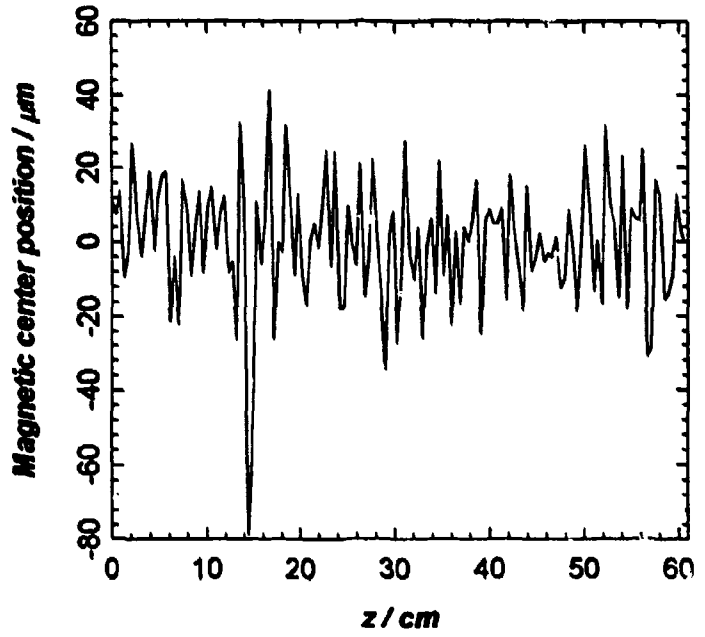

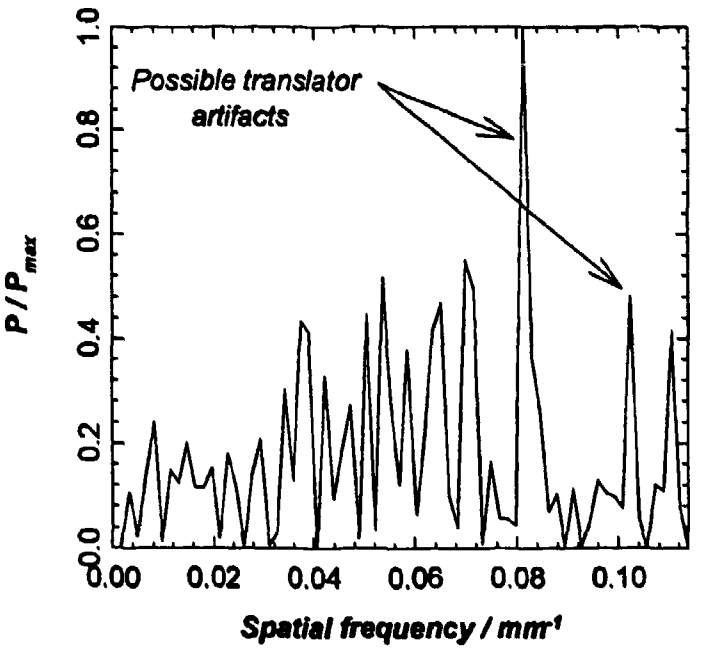

Figure 9. Stoner and Bekefi

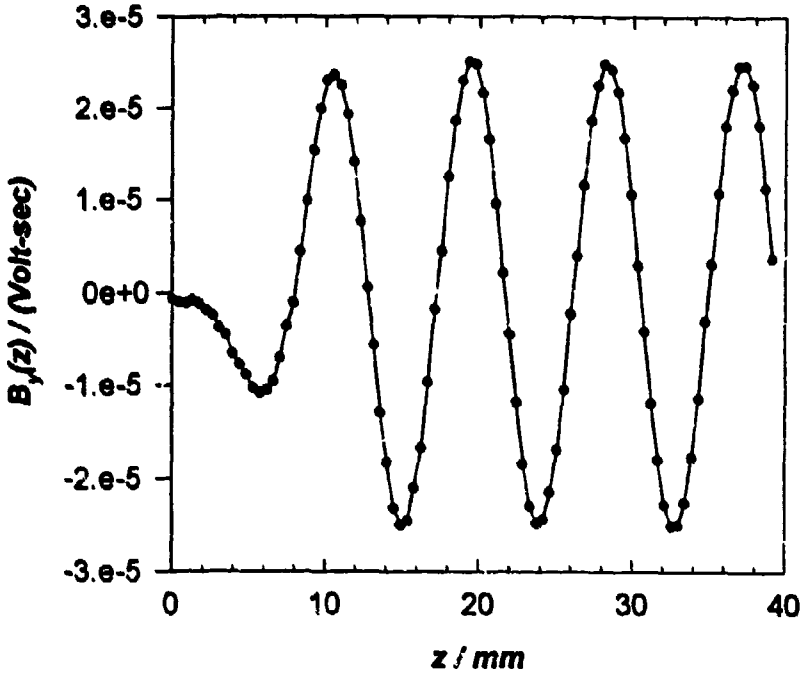

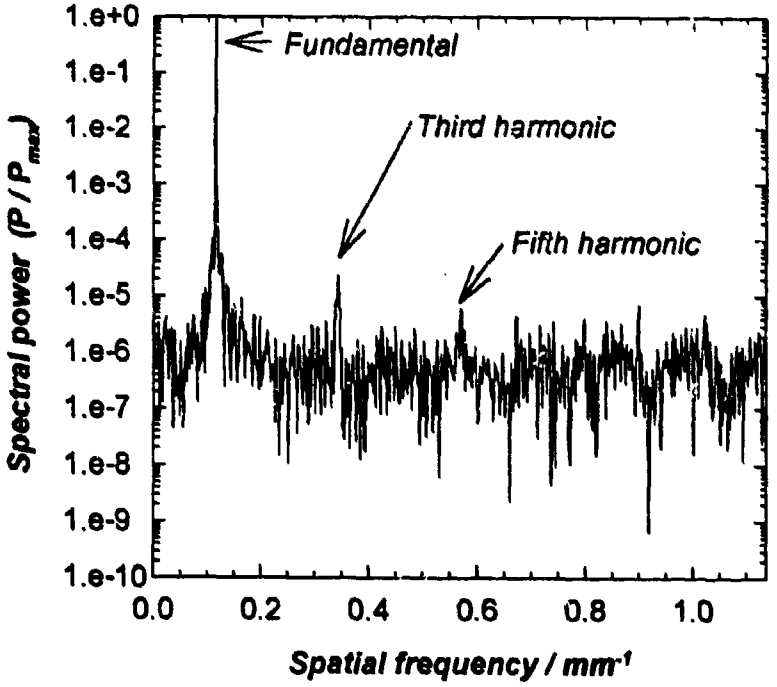

Figure 10. Stoner and Belkefi

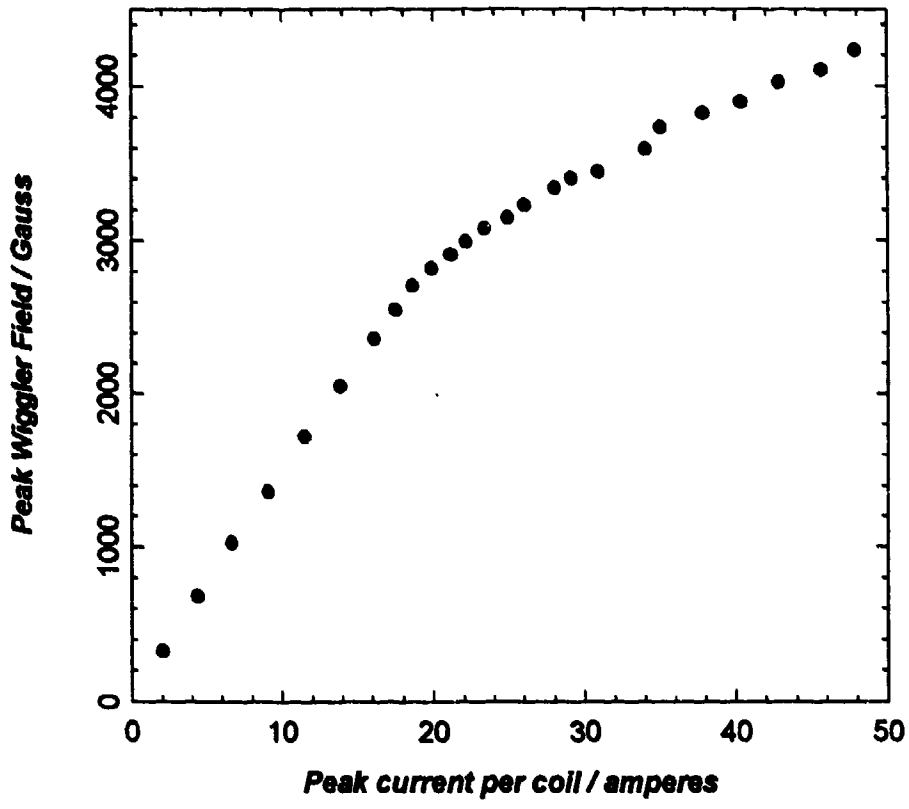

Figure 11. Stoner and Bekefi

Office of Naval Research

DISTRIBUTION LIST

Charles W. Roberson
Scientific Officer

Code: 1112AI
Office of Naval Research
800 North Quincy Street
Arlington, VA 22217

3 copies

Administrative Contracting Officer
E19-628
Massachusetts Institute of Technology
Cambridge, MA 02139

1 copy

Director
Naval Research Laboratory
Washington, DC 20375
Attn: Code 2627

1 copy

Defense Technical Information Center
Bldg. 5, Cameron Station
Alexandria, VA 22314

2 copies